WALAILAK JOURNAL
http://wjst.wu.ac.th Article

First Principles Study of the Electronic Structure, Structural Properties and Superconductivity of Nickel Hydride

Shunmugam KANAGAPRABHA[1], Asvini MEENAATCI[2], Ratnavelu RAJESWARAPALANICHAMY[2] and Kombiah IYAKUTTI[3]

[1]*Department of Physics, Kamaraj College, Tuticorin, Tamil Nadu 628003, India*
[2]*Department of Physics, Nadar Mahajana Sangam S. Vellaichamy Nadar College, Madurai, Tamil Nadu 625019, India*
[3]*School of Physics, Madurai Kamaraj University, Tamil Nadu 625021, India*

(Corresponding author; e-mail: rrpalanichamy@gmail.com)

Received: 15 January 2012, Revised: 18 February 2012, Accepted: 4 April 2012

Abstract

First principles calculations are performed using a tight-binding linear muffin-tin orbital (TB-LMTO) method with local density approximation (LDA) and atomic sphere approximation (ASA) to understand the electronic properties of nickel hydride. The equilibrium geometries, the electronic band structure, the total and partial density of states (DOS) are obtained under various pressures and are analyzed in comparison with the available experimental and theoretical data. The most stable structure of NiH is the NaCl structure, NiH_2 the CaF_2 structure and NiH_3 the AlH_3 structure at normal pressure. Our result indicates that the maximum storage capacity achieved is 4.9 % for NiH_3. In particular there is no superconductivity in NiH. An increase in T_c is predicted due to the addition of H atoms. The obtained T_c values for NiH_2 and NiH_3 are 5 K and 10 K respectively at normal pressure. Also, it is found that the superconducting transition temperature (T_c) increases as the pressure increases.

Keywords: Ab initio calculations, electronic structure, phase transition, mechanical properties, superconductivity

Introduction

Many transition metals react readily with hydrogen to form stable metal hydrides [1]. Metal hydrides are of intense scientific and technological interest in the view of their potential application, e.g., for hydrogen storage, in fuel cells and internal combustion engines, as electrodes for re-chargeable batteries and in energy conversion devices. Hydrides for hydrogen storage must form hydrides with a high hydrogen to-metal mass ratio, but should not be too stable, so that the hydrogen can easily be released without excessive heating [2]. A number of interesting modifications is produced in the metallic characteristics when hydrogen is added. Wimmer [3] discussed the growing importance of computations in materials science. Most transition metals form hydrides at sufficiently high pressures of hydrogen [4]. Wolf and Baranowski [5] measured the heat capacity of nickel hydride. Eckert *et al*. [6] determined the optical phonon density of states in nickel hydride at room temperature using incoherent-inelastic neutron-scattering techniques. Cable *et al*. [7] performed coherent neutron scattering measurements to determine the crystal structure and hydrogen content of nickel hydride. Vargas and Christensen [8] presented a self-consistent calculation of the electronic structure of nickel hydride. Moreover, to the best of our knowledge, the structural phase transition, hydrogen storage capacity and superconducting transition temperature of nickel hydride have been not yet reported. Recently, Kim *et al*. [9] investigated the

superconductivity of ScH_3, LaH_3 and YH_3. Meanwhile, we have investigated the electronic structure and mechanical stability of MgH_2 [10]. In this paper, the band structure, the density of states (DOS), the electronic charge distribution and the structural phase transition of nickel hydride under various pressures are investigated by first principles calculation. All the possible cubic, tetragonal and hexagonal crystal systems are chosen as candidate structures of nickel hydride, including zinc blende (ZB) (space group $F\bar{4}3m$), NaCl and CaF_2 (space group Fm3m), CsCl (space group Pm3m), WC (space group $P\bar{6}m2$) and tetragonal (space group I4/mmm). Further, the superconducting transition temperature T_c of NiH, NiH_2 and NiH_3 is calculated by using the McMillan formula [11]. The hydrogen storage capacity of nickel is analyzed.

Computational details

To compute the electronic structure and the basic ground state properties of NiH, NiH_2 and NiH_3, TB-LMTO (tight-binding linear muffin-tin orbital method) has been used [12,13]. In the LMTO scheme, the crystal potential is approximated by a series of non-overlapping atomic like spherical potentials and a constant potential between the spheres. The Schrödinger equation can be solved in both regions. These solutions are then matched at the sphere boundaries to produce muffin-tin orbitals. These muffin-tin orbitals are used to construct a basis which is energy independent, linear order in energy and rapidly convergent. Each orbital must satisfy Schrödinger's differential equation in the region between the atoms. Here the potential is flat on a scale of 1 Ry and, since the energy range of interest begins near the point where the electron can pass between the atoms and extends upwards by about 1 Ry, it seems natural to choose orbital's which have zero kinetic energy, i.e., satisfy the Laplace equation, in the interstitial region. In the tight-binding muffin-tin orbital the solution of Schrödinger's equation is written as,

$$\left|\chi^{\alpha}(E)\right\rangle = \begin{cases} \left|\varphi(E)\right\rangle N^{\alpha}(E) + \left|J^{\alpha}\right\rangle P^{\alpha}(E) & r \le w \\ \left|K^{\alpha}\right\rangle & r \ge w \end{cases} \quad (1)$$

where, r is any distance from the centre of the muffin-tin sphere, w is the average Wigner-Seitz radius and α are dimensionless screening constants. Inside the MT sphere, the base field (or) unscreened field $\left|K\right\rangle$ is defined by

$$\left|K\right\rangle = \left|\varphi(E)\right\rangle N^{\alpha}(E) + \left|J^{\alpha}\right\rangle P^{\alpha}(E) \quad (2)$$

In the interstitial region, the screened field $\left|k^{\alpha}\right\rangle$ is defined by,

$$\left|k^{\alpha}\right\rangle = \left|\varphi(E)\right\rangle N^{\alpha}(E) + \left|J^{\alpha}\right\rangle P^{\alpha}(E) - \left|J^{\alpha}\right\rangle S^{\alpha} \quad (3)$$

where $\phi(E)$ is normalized to unity in its sphere such that $\left\langle \varphi(E)\dot{\varphi}(E)\right\rangle = 0$ and $\left\{\varphi(E)\dot{\varphi}(E)\right\} = -1$. J^{α} is the screen field radial function and S^{α} is the screened structure matrix. The elements of the diagonal matrices P and N are,

$$P^{\alpha}(E) = \frac{\{\varphi(E), k\}}{\{\varphi(E), J^{\alpha}\}} = \frac{P^{o}(E)}{1 - \alpha P^{o}(E)} \quad (4)$$

$$N^{\alpha}(E) = \frac{\{J^{\alpha}, k\}}{\{J^{\alpha}, \varphi(E)\}} = \left(\frac{w}{2}\right)^{1/2} P^{\alpha}(E)^{1/2} \quad (5)$$

The set of energy dependent MTO's $\left|\chi^{\alpha}(E)\right\rangle$, thus equals $\left|k^{\alpha}\right\rangle$ and $\left|k\right\rangle$; the linear combination $\left|\chi^{\alpha}(E)\right\rangle u^{\alpha}$, specified by a column vector u^{α}, is seen to be a solution of Schrödinger's equation at energy E for the MT potential if it equals the one center expansions $\left|\varphi(E)\right\rangle > N^{\alpha}(E)u^{\alpha}$ in the spheres, i.e., if the set of linear homogeneous equations $[P^{\alpha}(E) - S^{\alpha}]u^{\alpha} = 0$ has a proper solution. This is the generalization of the so-called tail cancellation or Kerringa-Kohn-Rostoker (KKR) condition.

The secular matrix $[P^{\alpha}(E) - S^{\alpha}]$ depends on the potential only through the potential functions along the diagonal and for the most localized set it

has the TB two center form with S^{α} playing the role of the transfer integrals.

The screened field $\left|k^{0}\right\rangle$ is given by the superposition of bare fields $\left|k^{0}\right\rangle$ and that the relationship between the bare and screened structure matrices is,

$$S^{\alpha} = S^{o}(1-S^{o})^{-1} \quad (6)$$

The expansion co-efficient S° forms a Hermitian matrix which is dimensionless and independent of the scale of the structure. This is the so-called (bare) canonical structure matrix.

The KKR equations have the form of an Eigen value problem if P^{α} is a linear function of E. This is true, if $\alpha = \gamma$ (potential parameter) in which case the effective two center Hamiltonian is,

$$H^{\gamma}{}_{ij} = C_i S_{ij} + \left(\sqrt{\Delta_i}\right) S^{\gamma}{}_{ij} \left(\sqrt{\Delta_i}\right) \quad (7)$$

For crystals, where the matrix inversion in Eq. (7) can be performed, one may obtain from S° (or) S^{α}.

To obtain an Eigenvalue when $\alpha \neq \gamma$, energy independent orbitals are needed. Now, $\left|\chi^{\alpha}(E)\right\rangle$ is independent of energy, in the interstitial region and in the spheres, its first energy derivative at E_{γ} will vanish. Therefore, the orbital base is,

$$\left|\chi^{\alpha}\right\rangle = \left|\varphi\right\rangle + \left|\dot{\varphi}^{\alpha}\right\rangle h^{\alpha} \quad (8)$$

In this base, the Hamiltonian matrices are,

$$\left\langle \chi \middle| H - E_{\gamma} \middle| \chi \right\rangle = h(1+oh) \quad (9)$$

$$(H-E)\left|\varphi(E)\right\rangle = 0 \quad (10)$$

$H - E_{\gamma}$ is the effective two center TB Hamiltonian. This has a shorter range. Therefore, this set of equations is used in self consistent calculations. In the interstitial region Eq. (9) becomes,

$$\left\langle \chi^{\alpha} \middle| H - E_{\gamma} \middle| \chi^{\alpha} \right\rangle = h^{\alpha}(1+o^{\alpha}h^{\alpha}) \quad (11)$$

The set of $\left|\chi^{\alpha}\right\rangle$ is thus complete to first order in $(E-E_{\gamma})$ and it can yield energy estimates correct to the third order. A Von-Barth and Hedin [14] parameterization scheme has been used for the exchange correlation potential within the local density approximation (LDA). The accuracy of the total energies obtained within the density functional theory, often using LDA, is in many cases sufficient to predict which structure at a given pressure has the lowest free energy [15]. The atomic sphere approximation (ASA) has been used in the present work. The Wigner-Seitz sphere is chosen in such a way that the sphere boundary potential is at its minimum and the charge flow is in accordance with the electronegativity criteria. The s, p and d partial waves are included. The tetrahedron method [16] of the Brillouin zone (k - space) integration has been used to calculate the density of states. The configurations of Ni $4s^2 3d^8$ and H $1s^1$ are treated as the valence electrons. Pressure calculations are done with second order Birch Murnaghan equation of states [17].

$$P = \frac{3}{2}B\left[\left(\frac{V_o}{V}\right)^{7/3} - \left(\frac{V_o}{V}\right)^{5/3}\right] \times \left\{1 + \frac{3}{4}(B' - 4)\left[\left(\frac{V_o}{V}\right)^{2/3} - 1\right]\right\} \quad (12)$$

where B and B′ are the bulk modulus and the first derivative of the bulk modulus respectively.

Results and discussion

Geometric and mechanical property

At ambient conditions nickel hydride crystallizes with a fcc structure in the space group Fm3m (225). The Wyckoff positions for the Ni and H atoms are 4a:(0,0,0) and 4b:(0.5,0.5,0.5) respectively and contains four formula units per unit cell. The primitive unit cells of NiH, NiH_2 and NiH_3 are shown in **Figure 1**.

Valence electron density (VED) is defined as the total number of valence electrons divided by volume per unit cell which is an important factor for analyzing super hard materials. The

equilibrium volume V_0 (Å^3), lattice parameters a (Å), c (Å), total energy (Ry), density of states (DOS) at the Fermi level $N(E_F)$ {DOS(States/Ry.Cell)}, radius of the Wigner-Seitz cell (Rwz), band energy E_B (Ry), Fermi energy E_F (Ry) obtained from the TB-LMTO method are listed in **Table 1**. The calculated VEDs are 0.698 electrons/Å^3 for ZB-NiH, 0.912 electrons/Å^3 for NaCl-NiH, 0.766 electrons/Å^3 for CsCl-NiH, 0.926 electrons/Å^3 for CaF_2-NiH_2, 0.621 electrons/Å^3 for hexagonal-NiH_2 and 0.455 electrons/Å^3 for tetragonal-NiH_2. It is worth noticing that all VEDs for NaCl-NiH and CaF_2-NiH_2 structure are similar to Ni metal (0.917 electrons/Å^3). The equilibrium volumes per formula unit are 15.761 Å^3 for ZB-NiH, 12.057 Å^3 for NaCl-NiH, 14.367 Å^3 for CsCl-NiH, 12.953 Å^3 for CaF_2-NiH_2, 19.336 Å^3 for Hexagonal NiH_2 and 26.364 Å^3 for Tetragonal NiH_2, which are higher than that of Ni metal (10.9 Å^3) due to the additional H atoms.

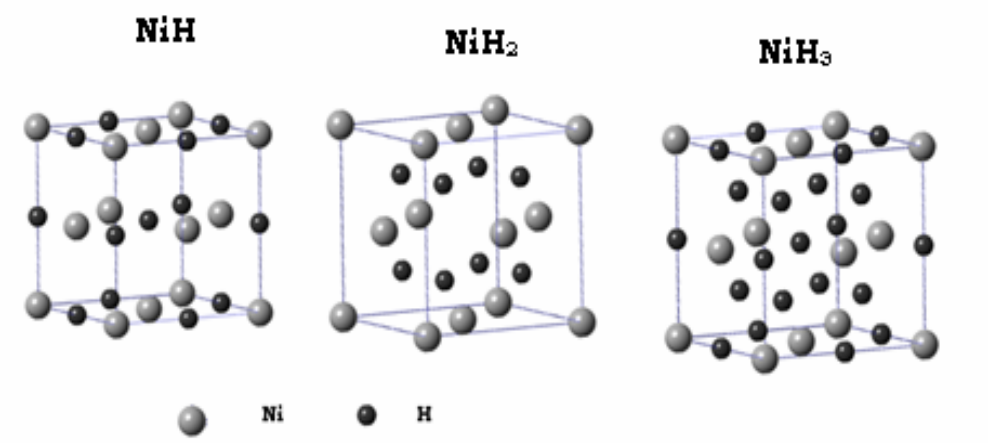

Figure 1 Primitive unit cells of NiH, NiH_2 and NiH_3.

Table 1 Equilibrium volume V_0 (Å^3), lattice parameters a(Å), c(Å), Valence electron density ρ (electrons/ Å^3),the radius of the Wigner-Seitz cell (Rwz), Fermi energy E_F (Ry), band energy E_B (Ry), density of states (DOS) at the Fermi level N (E_F) {DOS(States/Ry.Cell)} and total energy E(total) (Ry).

	NiH			**NiH_2**		
	NaCl	**CsCl**	**ZB**	**Cubic(CaF_2)**	**Tetragonal**	**Hexagonal**
V_0	12.057	14.367	15.761	12.953	26.364	19.336
a	3.64	2.431	3.98	3.728	3.93	2.734
	3.69 [8]			3.717 [7]		
c	-	-	-	-	3.414	2.987
ρ	0.912	0.766	0.698	0.926	0.455	0.621
R_{WZ}	2.134	2.263	1.852	1.735	1.825	1.983
E_F	0.009	–0.058	–0.010	0.299	–0.167	–0.072
E_B	–2.468	–2.671	–2.105	–1.384	–4.201	–3.696
$N(E_F)$	9.6290	16.2913	13.5624	0.0518	10.0398	9.6281
E(total)	–3038.89	–3038.82	–3038.86	–3040.02	–3039.87	–3039.96

Young's modulus E and Poisson's ratio are two important factors for technological and engineering applications. The Young's modulus, Poisson's ratio, bulk modulus and shear modulus are calculated using the following expressions:

$$E = \frac{9BG}{3B+G} \quad (13)$$

$$\upsilon = \frac{3B - 2G}{2(3B+G)} \quad (14)$$

$$B = -Vo\frac{dP}{dV} \quad (15)$$

$$G = \frac{C_{11} - C_{12}}{2} \quad (16)$$

The stiffness of the solid can be analyzed using the Young's modulus (E) value. Bulk modulus B, Young's modulus E (GPa), shear modulus G (GPa), Poisson's ratio υ and the elastic constants C_{11}, C_{12} and C_{44} (GPa) are calculated for NaCl-NiH which is more stable than the other phases and are listed in **Table 2**.

The elastic constants C_{ij} should satisfy the well known Born-Huang criteria for the stability of cubic crystals [18].

$$C_{44} > 0,\ C_{11} > |\ C_{12}\ |,\ C_{11} + 2C_{12} > 0 \quad (17)$$

From **Table 2**, it is seen that the obtained elastic constants of cubic NaCl-NiH satisfy the Born-Huang criteria, suggesting that it is mechanically stable. The computed elastic moduli are in agreement with the available theoretical data [3]. The Young's modulus of Ni is calculated as 254 GPa by Erich Wimmer [3]. It is found that the Young's modulus of NiH is less than Ni. It shows that the stiffness of NiH is less than Ni. Poisson's ratio reflects the stability of the crystal against shear. The ratio can formally take values between −1 and 0.5, which corresponds to the lower limit, when the volume remains unchanged. The obtained Poisson's ratio of NaCl-NiH is 0.4. Hence, the NaCl – NiH is stable at normal pressure.

Table 2 Elastic moduli and elastic constants for NaCl-NiH.

B GPa	**G GPa**	**E GPa**	**υ**	**C_{11} GPa**	**C_{12} GPa**	**C_{44} GPa**
212.64	45	126.1	0.4	272.64	182.64	45
198 [3]	41 [3]	116 [3]				

Electronic structure

The band structure of nickel hydrides is computed for various reduced volumes and the band structures for the reduced volume $V/V_0 = 1.0$ and 0.4 are given in **Figure 2**. From **Figure 2**, it is seen that, at normal pressure, the band structure has 6 valence bands (bottom most) corresponding to 11 valence electrons which comes from $4s^2 3d^8$ of the Ni atom and $1s^1$ state electrons of the H atom. Above the Fermi level the empty conduction bands are present with mixed s, p, and d characters. The empty conduction bands are highly overlapping with the valence bands and there is no band gap. Hence, at normal pressure, nickel hydride is a metal. At high pressure the bands get dispersed.

To understand the correlation between the electronic and mechanical properties, we have computed the density of states under equilibrium geometries. The total DOS of NiH, NiH_2 and NiH_3 are shown in **Figure 3**. From **Figure 3**, it is observed that, the spike near −0.5 Ry. is due to s state electrons of the H atom. The highest spike near the Fermi level is expected to be essentially Ni 3d-like states. The Fermi level is shifted by adding the H atoms one by one.

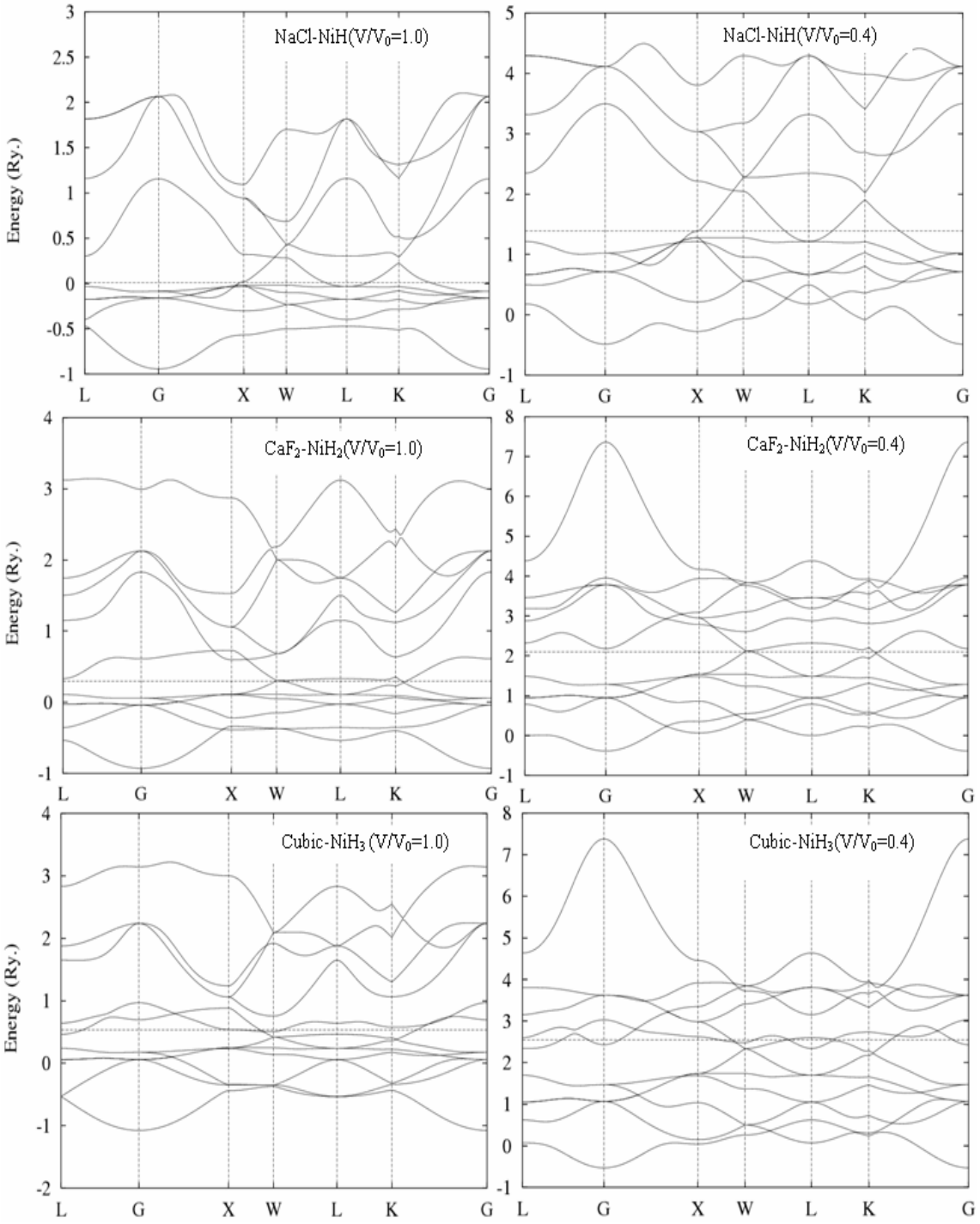

Figure 2 Band structures of nickel hydrides at $V/V_0 = 1.0$ and 0.4.

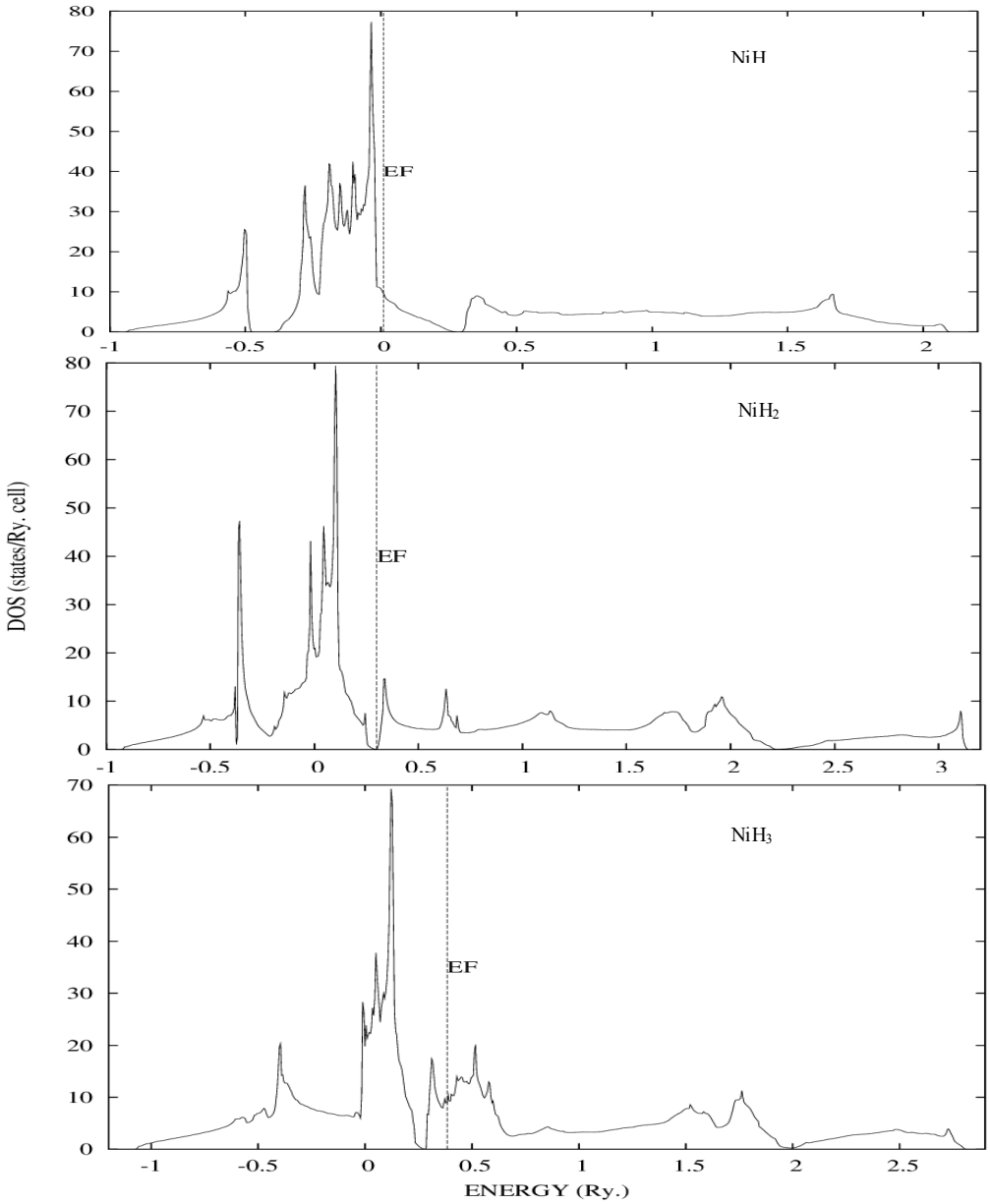

Figure 3 Total density of states of NiH, NiH_2 and NiH_3 at normal pressure.

Electrons in the s, p and d shells of Ni and H at different pressures for NaCl-NiH are given in **Table 3**. From **Table 3**, it is found that as the pressure increases, a fraction of 4s state electrons are transferred to 4p and 3d states of the Ni atom. Similarly a portion of 1s electrons are transferred to 2p and 3d states of the H atom.

The partial DOS of NaCl-NiH is shown in **Figure 4**.

Table 3 Electrons in s, p and d shells of Ni and H at different pressures for NaCl-NiH.

P (GPa)	Ni			Q-valence	H			Q-valence
	$4s^2$	$4p^0$	$3d^8$		$1s^2$	$2p^0$	$3d^0$	
Normal	0.521	0.747	8.776	10.044	0.742	0.181	0.033	0.956
45.158	0.512	0.788	8.736	10.036	0.729	0.198	0.037	0.964
138.167	0.497	0.822	8.704	10.023	0.719	0.217	0.041	0.977
406.324	0.465	0.846	8.701	10.010	0.711	0.231	0.046	0.988

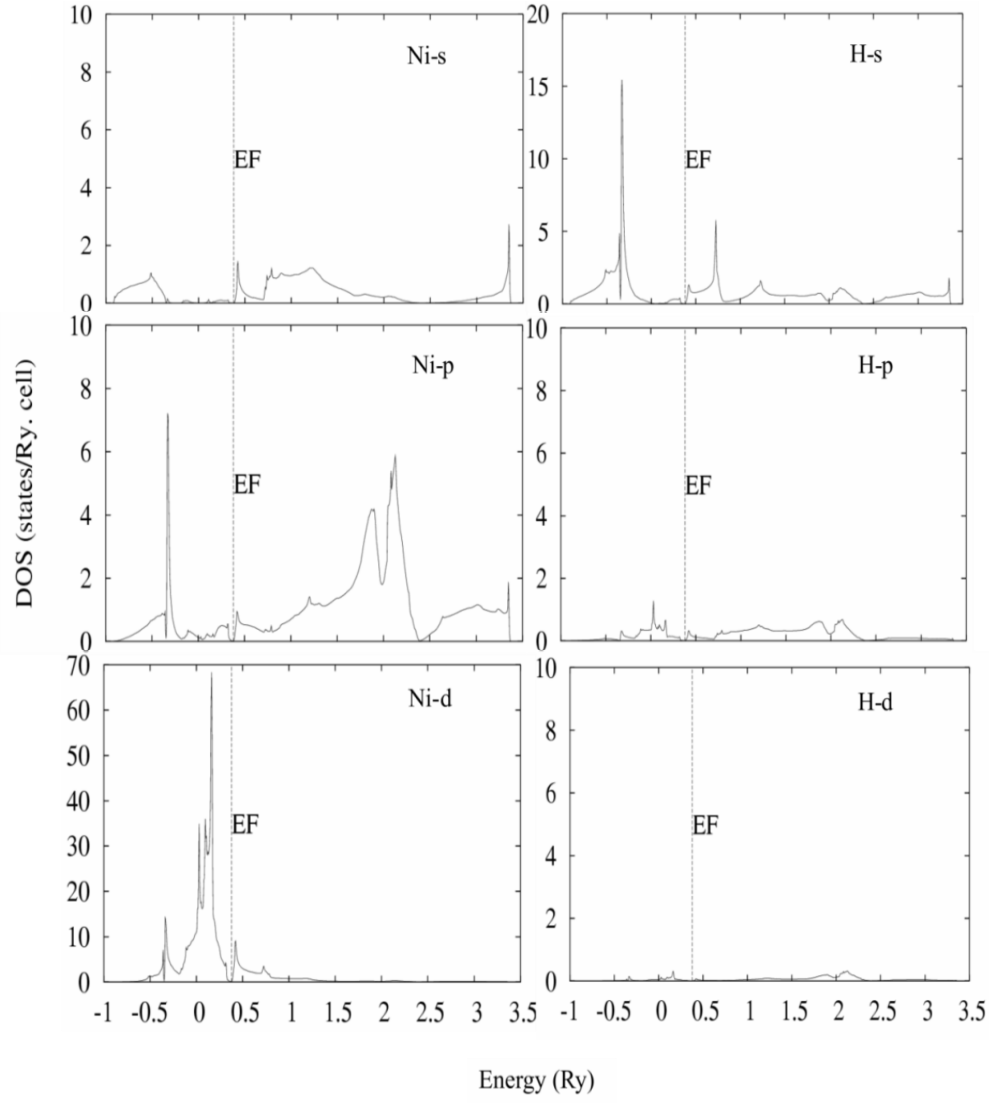

Figure 4 Partial density of states of NiH at normal pressure. Vertical dotted line indicates the Fermi level.

It is observed that the electrons from the p and d state electrons of the Ni and H atoms contribute much to the DOS in the lower-energy region. The highest spike is due to the 3d state electrons of Ni atom. As the pressure increases, the height of the spike decreases. The charge density distribution for NaCl-NiH is shown in **Figure 5**. It is clearly seen that charge strongly accumulates between the Ni and H atoms, which means that a strong directional bonding exists between them.

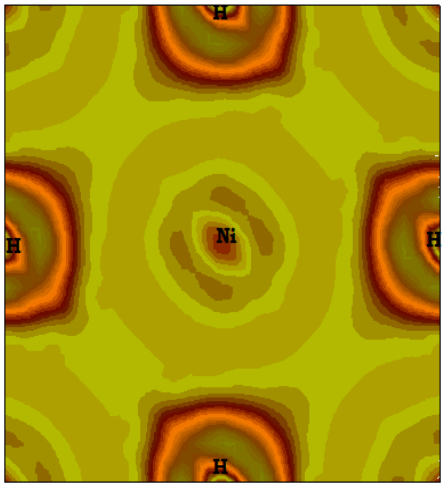

Figure 5 Charge density plot of NaCl-NiH at normal pressure.

Energetics and phase diagram

The energy-V/V_0 curves corresponding to the three different phases of NiH and NiH_2 are shown in **Figures 6** and **7**, where V/V_0 is the ratio between the volume at any pressure and the equilibrium volume. It is observed that at normal pressure, the thermodynamically stable phase of NiH and NiH_2 are NaCl and CaF_2 structures respectively. A pressure induced structural phase transition from NaCl phase to ZB phase is observed for NiH and CaF_2 to a tetragonal phase is observed for NiH_2.

In order to calculate the transition pressure, the Gibb's free energy is calculated for the two phases using the expression.

$$G = E_{tot}+PV-TS \quad (18)$$

Since the theoretical calculations are performed at 0 K, the Gibb's free energy will be equal to the enthalpy (H)

$$H = E_{tot} + PV \quad (19)$$

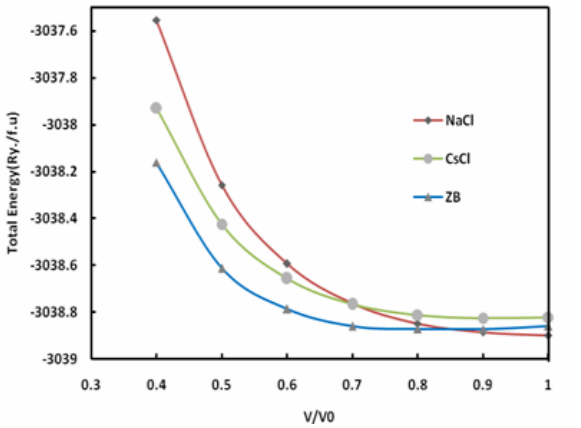

Figure 6 Structural phase transition between the different phases of NiH.

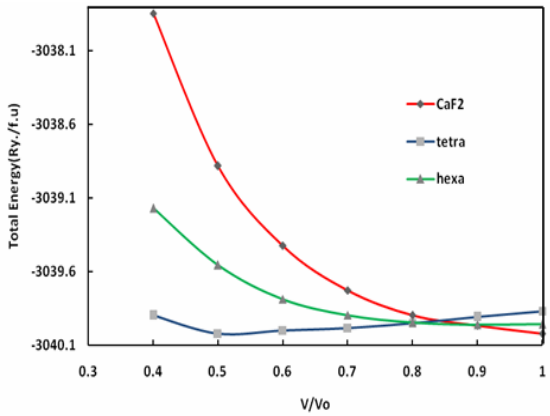

Figure 7 Structural phase transition between different phases of NiH_2.

At a given pressure, a stable structure is one in which the enthalpy has its lowest value. The transition pressures are calculated at which the enthalpies of the two phases are equal. The enthalpy versus pressure plots of NiH and NiH_2 are shown in **Figures 8** and **9**. From **Figure 8**, it is seen that, there is a phase transition from the NaCl to ZB phase at a pressure of 24 GPa. Similarly, from **Figure 9**, a phase transition is found from CaF_2 to tetragonal phase at a pressure of 64 GPa.

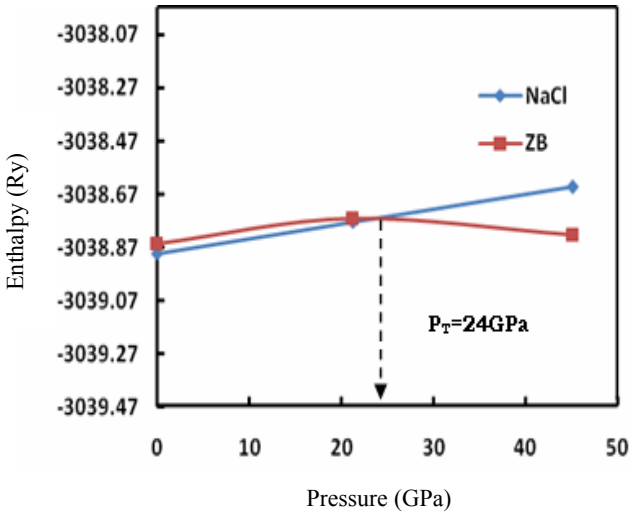

Figure 8 Enthalpy versus pressure curve of NiH.

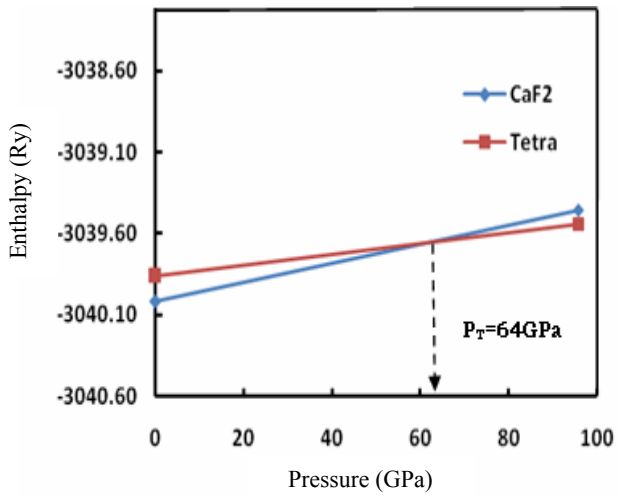

Figure 9 Enthalpy versus pressure curve of NiH_2.

Superconducting transition temperature (T_c K)

The superconducting transition temperature T_c of NiH, NiH_2 and NiH_3 are estimated using McMillan equation [11].

$$T_c = \frac{\theta_D}{1.45}\exp\left[\frac{1.04(1+\lambda)}{\lambda-\mu^*(0.62\lambda)}\right] \quad (20)$$

where θ_D is the Debye temperature (in energy units) and μ^* is the electron-electron interaction parameter, which is estimated using the relationship,

$$\mu^* = \frac{0.26\,N(E_F)}{(1+N(E_F))} \quad (21)$$

The electron-phonon coupling constant

$$\lambda = \frac{N(E_F)<I^2>}{M<\omega^2>} \quad (22)$$

where N (E_F) is the density of states at the Fermi level , $<I^2>$ is the square of the electron phonon matrix element averaged over the Fermi energy.

$$<I^2> = 2\sum_l \left\{\frac{(l+1)}{2l+1)(2l+3)}\right\} M^2_{l,l+1} \left\{\frac{N_l(E_F)N_{l+1}(E_F)}{N(E_F)^2}\right\} \quad (23)$$

$<\omega^2>$ is the average of the phonon frequency squared and M is the atomic mass.

$$<\omega^2> = 0.5\ \theta_D{}^2 \quad (24)$$

The computed values of λ, μ^* and T_c as a function of pressure for NiH, NiH_2 and NiH_3 are given in **Table 4**. The estimated superconducting transition temperature (T_c) is 1.52 K for NiH. The T_c value increases with an increase in pressure. The computed superconducting transition temperature for the normal pressure is compared with the available theoretical work [19]. Thus, our results conclude there is no superconductivity in NiH at normal pressure. But, it is found that due to the addition of hydrogen atoms, the superconducting transition temperature increases [20]. The estimated T_c for NiH_2 and NiH_3 are 5.5 K and 10 K at normal pressures respectively. For NiH_3, the T_c value at 578.4 GPa (V/V_0 = 0.6) is computed as 25.571 K. Hence the addition of hydrogen atoms increases the T_c value of nickel hydride. Also, it is found that the T_c value increases as the pressure increases.

Table 4 λ, μ^* and T_c values as a function of pressure for NiH, NiH_2 and NiH_3.

V/Vo	NiH			NiH_2			NiH_3		
	λ	μ^*	T_c (K)	λ	μ^*	T_c (K)	λ	μ^*	T_c (K)
1.0	0.427	0.107	1.528	0.380	0.006	5.557	0.782	0.132	10.018
0.8	0.4725	0.100	1.633	0.578	0.095	6.130	0.869	0.088	16.737
0.6	0.508	0.0697	1.887	0.756	0.089	7.561	0.964	0.084	25.571

Hydrogen storage in nickel hydride

Hydrogen fuel, which can be readily produced from renewable energy sources, contains at least three times larger chemical energy per mass 142 MJ Kg than any chemical fuel, thus making a hydrogen fuel cell an attractive alternative to the internal combustion engine for transportation [21]. Elements, especially those in group I - IV and some transition metals, have their hydride and amide\imides forms. There is, therefore, still plenty of scope for further exploring metal-H system for hydrogen storage. In our study, we have analyzed the storage capacity of Ni by adding hydrogen atoms one by one. The formation energy, density of H/unit cell and storage capacity of NiH, NiH_2 and NiH_3 is given in **Table 5**. From the table, we see that the formation energy for NiH, NiH_2 and NiH_3 are negative. It shows that the formation is possible. The highest hydrogen storage obtained for NiH_3 is 4.9 %.

Table 5 Storage capacity of hydrogen in Ni.

	Formation Energy	Density of H/unit cell	Weight % of Hydrogen
NiH_1	–0.17	9.7	1.6
NiH_2	–0.25	19.4	3.3
NiH_3	–0.15	29.1	4.9

Conclusion

The band structure, density of states, structural phase transition, charge density and superconducting transition temperature under various pressures are investigated based on first principles calculation under the framework of tight-binding theory within the local density approximation. At normal pressure, the thermodynamically stable phase of NiH is the NaCl structure and for NiH_2, the CaF_2 phase is more stable. At certain high pressures, it is found that a structural phase transition occurs from NaCl to ZB for NiH and from CaF_2 to a tetragonal phase for NiH_2. Electronic structure calculations show that NiH presents obvious metallic features. Our results conclude, that there is no superconductivity in NiH. But, due to the addition of hydrogen atom we observe superconductivity in NiH_2 and NiH_3. The estimated T_c values for NiH_2 and NiH_3 are 5.5 K and 10 K respectively. Also, it is found that as the pressure increases, the T_c value also increases in NiH, NiH_2 and NiH_3. The maximum hydrogen storage capacity achieved is 4.9 % for NiH_3. We hope that this work can stimulate further experimental research on nickel hydride.

Acknowledgements

We thank our college management for their constant encouragement. The financial assistance from UGC (MRP. F.No-38-141/2009), India is duly acknowledged with thanks.

References

[1] Y Fukai. *Metal Hydrogen System: Basics Bulk Properties*. Springer, Berlin, 2005.
[2] P Vajeeston, P Ravindran, A Kjekshus, and H Fjellvåg. Structural stability of BeH_2 at high pressures. *Appl. Phys. Let.* 2004; **84**, 34-6.
[3] E Wimmer. The growing importance of computations in materials science. Current capabilities and perspectives. *Mat. Sci.* 2005; **23**, 325-44.
[4] VE Antonov. Phase transformations, crystal and magnetic structures of high-pressure hydrides of *d*-metals. *J. Alloy. Comp.* 2002; **330-332**, 110-6.
[5] G Wolf and B Baranowski. Specific heat of nickel hydride from 10 to 200 K. *J. Phy. Chem. Solid.* 1971; **32**, 1649-55.
[6] J EcKert, CF Majkzrak and LP WB Daniels. Optic phonons in nickel hydride. *Phys. Rev. B.* 1984; **29**, 3700-2.
[7] JW Cable, EO Wollan and WCK Le. The crystal structure of nickel hydride. *Journal De Physique.* 1964; **25**, 460.
[8] P Vargas and NE Christensen. Band-structure calculations for Ni, Ni_4H, Ni_4H_2, Ni_4H_3, and NiH. *Phys. Rev. B.* 1987; **35**, 1993-2004.
[9] DY Kim, RH Scheicher, HK Mao, TW Kang and R Ahuja. General trend for pressurized superconducting hydrogen-dense materials. *Proc. Natl. Acad. Sci.* 2010; **107**, 2793-6.
[10] S Kanagaprabha, ATA Meenaatci, RR Palanichamy and K Iyakutti. First principles study of pressure induced structural phase transition in hydrogen storage material-MgH_2. *Physica B* 2012; **407**, 54-9.
[11] WL McMillan. Transition temperature of strong-coupled superconductors. *Phys. Rev.* 1968; **167**, 331-44.
[12] OK Anderson. Linear methods in band theory. *Phys. Rev.* B. 1975; **12**, 3060-83.
[13] HL Skriver. *The LMTO Method*. Springer, Heidelberg, 1984.
[14] U von Barth and L Hedin. A local exchange-correlation potential for the spin polarized case. *J. Phys. C*: *Solid State Phys*. 1972; **5**, 1629-42.
[15] NE Christensen, DL Novikov, RE Alonso and CO Rodriguez. Solids under Pressure. Ab Initio Theory. *Phys. Status Solidi* 1999; **211**, 5-16.
[16] O Jepsen and OK Anderson. The electronic structure of h.c.p. Ytterbium. *Solid State Commun.* 1971; **9**, 1763-7.
[17] F Birch. Finite elastic strain of cubic crystals. *Phys. Rev.* 1947; **71**, 809-24.
[18] M Born and K Huang. *Dynamical Theory of Crystal Lattices*. Clarendon, Oxford, 1956.
[19] M Gupta and JP Burger. The electronic structure and its relationship to superconductivity in NiH. *J. Phys. F.* 1980; **10**, 2649-64.
[20] NI Kulikov, VN Borzunov and AD Zvonkov. The electronic band structure and interatomic bond in nickel and titanium hydrides. *Physica Status Solidi* 1978; **86**, 83-91.
[21] L Schlapbach and A Zuttel. Hydrogen-storage materials for mobile applications. *Nature* 2001; **414**, 353-8.